

---

**Obese neuronal PPAR $\gamma$  knock-out mice are leptin sensitive but show impaired glucose tolerance and fertility**

Marina O. Fernandez, Shweta Sharma, Sun Kim, Emily Rickert, Katherine Hsueh, Vicky Hwang, Jerrold M. Olefsky and Nicholas J.G. Webster

*Endocrinology*  
Endocrine Society

Submitted: November 04, 2016

Accepted: November 04, 2016

First Online: November 14, 2016

---

Early Release articles are PDF versions of manuscripts that have been peer reviewed and accepted but not yet copyedited. The manuscripts are published online as soon as possible after acceptance and before the copyedited, typeset articles are published. They are posted "as is" (i.e., as submitted by the authors at the modification stage), and do not reflect editorial changes. No corrections/changes to the PDF manuscripts are accepted. Accordingly, there likely will be differences between the Early Release manuscripts and the final, typeset articles. The manuscripts remain listed on the Early Release page until the final, typeset articles are posted. At that point, the manuscripts are removed from the Early Release page.

---

DISCLAIMER: These manuscripts are provided "as is" without warranty of any kind, either express or particular purpose, or non-infringement. Changes will be made to these manuscripts before publication. Review and/or use or reliance on these materials is at the discretion and risk of the reader/user. In no event shall the Endocrine Society be liable for damages of any kind arising references to, products or publications do not imply endorsement of that product or publication.

## Obese neuronal PPAR $\gamma$ knock-out mice are leptin sensitive but show impaired glucose tolerance and fertility

Marina O. Fernandez<sup>2,4</sup>, Shweta Sharma<sup>2</sup>, Sun Kim<sup>2</sup>, Emily Rickert<sup>2</sup>, Katherine Hsueh<sup>2</sup>, Vicky Hwang<sup>2</sup>, Jerrold M. Olefsky<sup>2</sup> and Nicholas J.G. Webster<sup>1,2,3</sup>

<sup>1</sup>Medical Research Service, VA San Diego Healthcare System, San Diego CA 92161 <sup>2</sup>Department of Medicine, School of Medicine and <sup>3</sup>Moore's Cancer Center, University of California San Diego, La Jolla, CA, 92093.

Received 4 November 2016. Accepted 4 November 2016.

### Neuronal PPAR $\gamma$ deletion impairs fertility

<sup>4</sup>Current address: Laboratory of Neuroendocrinology, Instituto de Biología y Medicina Experimental, CONICET. Vuelta de Obligado 2490, C1428ADN, Buenos Aires, Argentina

PPAR $\gamma$  is expressed in the hypothalamus in areas involved in energy homeostasis and glucose metabolism. In this study, we created a deletion of PPAR $\gamma$  (BKO) in mature neurons in female mice to investigate its involvement in metabolism and reproduction. We observed that there was no difference in age at puberty onset between female BKO and littermate controls, but the BKO mice gave smaller litters when mated and fewer oocytes when ovulated. The female BKO mice had regular cycles but showed an increase in the number of cycles with prolonged estrus. The mice also had increased LH levels during the LH surge and histological examination showed hemorrhagic corpora lutea. The mice were challenged with a 60% high fat diet. Metabolically the female BKO mice showed normal body weight, glucose and insulin tolerance, and leptin levels but were protected from obesity-induced leptin resistance. The neuronal knockout also prevented the reduction in estrous cycles due to the HFD. Examination of ovarian histology showed a decrease in the number of primary and secondary follicles in both genotypes due to the HFD, but the BKO ovaries showed an increase in the number of hemorrhagic follicles. In summary, our results show that neuronal PPAR $\gamma$  is required for optimal female fertility, but is also involved in the adverse effects of diet-induced obesity by creating leptin resistance potentially through induction of the repressor *Socs3*.

## INTRODUCTION

Thiazolidinediones (TZDs) are a class of drugs that activate the nuclear receptor PPAR $\gamma$  and improve blood glucose control and insulin sensitivity in patients with type 2 diabetes mellitus (T2DM) (1). TZDs also induce weight gain in humans and rodent models not only by promoting adipogenesis and fluid retention but also by increasing food intake (2;3). Consistent with this, PPAR $\gamma$  is expressed in key brain areas involved in energy homeostasis and glucose metabolism (4). We have previously shown that neuronal PPAR $\gamma$  increases weight gain in male mice when placed on a high-fat diet (HFD), mediates the HFD-induced hypothalamic leptin resistance, and is required for the improvement of liver insulin sensitivity upon rosiglitazone treatment (5). Food intake and energy homeostasis are controlled by the hypothalamic melanocortin circuit in the arcuate nucleus (ARC) involving neuropeptide Y (NPY), proopiomelanocortin (POMC), agouti-related peptide (AgRP), and cocaine and amphetamine-regulated transcript (CART) expressing neurons (6). Insulin and leptin inhibit NPY/AGRP neurons and activate POMC/CART neurons to suppress food intake and increase energy expenditure integrating central and peripheral metabolism (7). Obesity causes both hypothalamic insulin (8) and leptin resistance (9) and also causes inflammation peripherally and in the hypothalamus (10;11).

Gonadotropin-releasing hormone (GnRH) is the central regulator of the hypothalamic-pituitary-gonadal (HPG) axis that controls mammalian reproductive function (12). It is released from the median eminence of the hypothalamus in a pulsatile manner and acts on anterior pituitary gonadotropes to stimulate the synthesis and release of follicle stimulating hormone (FSH) and luteinizing hormone (LH) (13). GnRH neuronal activity is controlled by kisspeptin release from *Kiss1* neurons in the ARC and anteroventral periventricular (AVPV) nuclei (14), and kisspeptin signaling is an essential regulator of fertility and puberty in numerous mammalian species, including humans (15;16). Interestingly, *Kiss1* neurons arise from POMC progenitor cells (17) and activation of *Kiss1* neurons triggers glutamatergic signaling to POMC and AGRP neurons leading to depolarization or hyperpolarization, respectively (18). NPY/AGRP neurons inhibit (19) but POMC/CART neurons stimulate the HPG axis (20) and melanocortin fibers make synaptic contact with *Gnrh1* and *Kiss1* neurons. Leptin is essential for pubertal development and mice lacking either leptin (*ob/ob*) or its receptor (*db/db*) are infertile in addition to being obese (21;22). The effects of leptin on fertility seem to be mediated by AgRP as ablation of AgRP neurons restores fertility in the *db/db* mice, and AgRP overexpression impairs fertility (23). While the effects of leptin on puberty are well documented, the lack of pubertal development in knockout mice has hindered studies of leptin's effects on adult fertility (21;22).

The role of PPAR $\gamma$  in the regulation of reproduction is less clear. Previously PPAR $\gamma$  was reported to influence reproduction, acting in either the pituitary or the ovary (24;25). Genetic studies have linked polymorphisms in PPAR $\gamma$  to polycystic ovary syndrome (PCOS), suggesting a connection between PPAR $\gamma$  activation and HPG axis function (26;27). PCOS is the major cause of anovulation and infertility and affects 5–10% of women of reproductive age (28). One of the characteristics of PCOS is increased circulating luteinizing hormone (LH) and normal or decreased follicle-stimulating hormone (FSH) levels (29;30). Alterations in LH pulses have also been observed suggesting a hypothalamic or a pituitary defect. TZD therapy in PCOS decreases serum LH and androgen levels, and increases ovulation rate (31). Although these drugs are known to have insulin-sensitizing effects, the mechanism underlying the action on the HPG axis is not understood. Clinical studies by Mehta et al. (32) showed that pioglitazone therapy reduces the amplitude of serum LH response but not the GnRH dose response, indicating that pituitary response is altered in-vivo. This could be a direct effect of TZDs on the pituitary as we have previously published that PPAR $\gamma$  impairs GnRH signaling in immortalized pituitary gonadotropes, and loss of PPAR $\gamma$  causes elevated LH (33) or an indirect effect resulting from changes in circulating androgens. Furthermore PPAR $\gamma$  action in the ovary is also important for ovulation (25). In this study we deleted PPAR $\gamma$  in neurons to investigate the role of neuronal PPAR $\gamma$  in metabolism and reproduction in female mice.

## METHODS

### *Animals:*

Male *Pparg*flox/flox mice (34;35) were bred with female *Syn1-Cre* mice (36) to generate female *Pparg*flox/+*:Cre* mice, which were then bred to *Pparg*flox/flox male mice to obtain *Pparg*flox/flox:*Cre* mice (referred to as BKO) and *Pparg*flox/flox littermate controls (referred to as Flox). The *Syn-Cre* allele was always maintained on the female side as *Syn-Cre* expresses in the testis (37). *Syn-cre* mice express the cre transgene as early as e12.5 in differentiated neurons throughout the brain (36). Recombination has been observed in neurons in the CA3 and DG of the hippocampus, layers IV/V of the cortex, cerebellum, thalamus, brain stem, and in multiple hypothalamic nuclei including the arcuate, dorsal medial, ventral medial, paraventricular and suprachiasmatic nucleus (38-40). However the transgene has been reported to have only limited expression in NPY and POMC neurons in the ARC, and in CA1 neurons in the hippocampus

(39;40). Mice were housed in a 12-h light, 12-h dark cycle. Males and females had access to standard chow and water ad libitum. At 15 weeks of age, cohorts of female and male mice were fed either a 60% high-fat diet (HFD, Research Diets D12492) or a 10% low-fat diet (LFD, Research Diets 12450B). Major lipid components of the HFD are derived from lard and include 20% palmitic acid, 11% stearic acid, 34% oleic acid, and 29% linoleic acid, resulting in 32% saturated fat, 36% monounsaturated and 32% polyunsaturated fat. Food intake and body weight were measured weekly. Mouse procedures conformed to the Guide for Care and Use of Laboratory Animals of the US National Institutes of Health and were approved by the Institutional Animal Use and Care Committee of UCSD.

***Puberty onset and fertility assessment:***

Male and female pups were weaned at 21 days of age. Weights were recorded daily from 21 to 37 days of age for both sexes. Female pups were checked for vaginal opening as a sign of onset of puberty. Six- to eight-week old BKO and Flox mice were paired in different combinations and bred over a period of six months. Average days before the first litter and average number of pups born to the indicated breeding pairs were recorded and analyzed. Estrous cycles were monitored in female mice by vaginal cytology for 3 weeks starting at 12 weeks of age, or after 6, 12 or 20 weeks on diets. Ovulation was assessed by superovulating mice using a PMSG/hCG protocol (5IU of PMSG s.c. followed 48 hours later by 5 IU of hCG s.c.). Mice were killed 16 hours post hCG and the oocytes were harvested from the oviducts and counted manually under a light microscope (41).

***Tissue collection and histology:***

Ovaries, brain, pituitaries and other tissues were harvested at sacrifice for both histology and RNA extraction. Paraffin embedded sections (5  $\mu$ m) were cut, dewaxed, and stained with hematoxylin and eosin. Follicle number and stage, and corpora lutea number were counted on 3-5 sections from ovaries from 3-4 mice per group and are presented as mean number per ovary (42). Follicle stages were defined as follows: 1<sup>o</sup> as having a single layer of cuboidal granulosa cells (GCs), 2<sup>o</sup> as having 2 or more layers of cuboidal GCs but no antrum, early antral as having small patches of clear space between GCs, antral as having clearly defined antrum, atretic as having irregular oocyte morphology. Ovarian sections examined were separated by 25  $\mu$ m. Images were scanned using Aperio ImageScope and analyzed using the Imagescope software (Leica).

***Gene expression:***

Total RNA was extracted from the tissues using RNAbee (Tel-Test Inc.) and RNA purification kits from QIAGEN or Macherey-Nagel following the manufacturers' instructions. First-strand cDNA was synthesized using a High Capacity cDNA synthesis kit (Applied Biosystems). Quantitative PCR (QPCR) assays were run in 20  $\mu$ L triplicate reactions on a MJ Research Chromo4 instrument or in 7 nl reactions on a BioMark™ HD System (Fluidigm). Gene expression levels were calculated after normalization to the housekeeping genes *m36B4*, *Gapdh* or *RpII*, using the  $2^{-\Delta\Delta Ct}$  method and expressed as relative mRNA levels compared to the control.

***Gonadotropin measurements:***

Blood (20  $\mu$ l) was collected from the tail vein of males and from females at diestrus and proestrus and plasma prepared. Plasma LH and FSH levels were measured by custom duplex Luminex assay based on the rat pituitary panel (catalog number RPT86K; Millipore Corp) in singlets. Sensitivity of the assay is as follows LH: 4.9 pg/mL and FSH: 47.7 pg/mL with an intra-assay coefficient of variation of 15%. After 6, 12 and 20 weeks on the diets, female mice were bled in the morning of diestrus and at the time of the proestrus surge (6 pm). Plasma LH and FSH levels were measured by Luminex assay (catalog number MPTMAG-49K). Sensitivity of

the assays was: LH 4.9 pg/mL; FSH 24.4 pg/mL. For the GnRH stimulation test, tail vein blood was collected before and 10 minutes after ip injection of 1  $\mu$ g/kg GnRH, and gonadotropins were measured.

***Intraperitoneal glucose tolerance and insulin tolerance tests:***

Female mice were subjected to i.p. glucose-tolerance tests after 17 weeks on diets and insulin-tolerance tests after 20 weeks. Mice were fasted for 6 hours starting at 6 am and then injected ip with glucose (1 g/kg body weight) or insulin (0.4 for LFD or 0.75 U/kg body weight for HFD). Tail vein blood glucose was measured at 0, 15, 30, 45, 60, 90, and 120 minutes after injection using a glucometer (OneTouch Ultra; Bayer Healthcare).

***Insulin, leptin and steroid measurements:***

Animals were fasted for 6 h. Fasting blood glucose concentration was measured on tail vein blood using a glucometer (OneTouch Ultra). Blood (50  $\mu$ l) was drawn from the tail vein in EDTA coated capillary tubes and plasma obtained by centrifugation at 4 °C. Fasting insulin and leptin were measured on plasma using the Mouse Metabolic Kit (Meso Scale Discovery, K15124C-2). Sensitivity of the assay was: leptin 43 pg/ml; insulin 15 pg/ml; CV 6% and 12% respectively. Estrogen, progesterone and testosterone were measured using a Custom Steroid Hormone Panel Kit (MSD). Sensitivity of the assay was: estradiol 5 pg/ml; progesterone 70 pg/ml; testosterone 20 pg/ml; CV 7%, 15% and 22% respectively.

***In vivo leptin sensitivity test:***

We measured food intake in individually housed mice injected with leptin (0.5 or 1 mg/kg intraperitoneally, National Hormone and Peptide Program, NHPP) at 12-h intervals for a total of four consecutive doses. Food intake and body weight were measured throughout the 48-h period and compared to a 48-h period during in which animals received twice daily i.p. injections of vehicle (PBS).

***Statistical analysis:***

Data was analyzed by 1-way or 2-way ANOVA followed by Tukey multiple comparison post-test, or Students t-test as appropriate using Prism (Graph Pad). Normality was assessed by D'Agostino-Pearson omnibus normality test. Results were expressed as Mean $\pm$ Standard Error and considered significant with  $p < 0.05$ .

## RESULTS

***Neuronal deletion of PPAR $\gamma$ :***

PPAR $\gamma$  was deleted from mature neurons by crossing *Pparg* floxed mice with mice expressing cre recombinase under control of the synapsin promoter (*syn-cre*) as published previously (5). Littermates that lacked the *syn-cre* allele were used as controls (Flox). Neuronal deletion was confirmed by PCR amplification of the recombined allele (Figure 1A). Recombination was observed in brain and also in testis, so the *cre* allele was always bred from the maternal side to prevent germline recombination. To verify brain-specific deletion of PPAR $\gamma$  in BKO mice, we isolated RNA from brain regions and from peripheral tissues for measurement of PPAR $\gamma$  mRNA abundance. *Pparg* expression was quantified by QPCR. There was a significant reduction in *Pparg* gene expression in the hypothalamus, but not in other tissues (Figure 1B). Surprisingly the expression was not reduced in whole brain but *Pparg* is also expressed in astrocytes that may mask changes in expression in neurons. Immuno-histochemical staining for PPAR $\gamma$  protein showed reduced staining in cortical slices in the BKO brain compared to the Flox controls (Figure 1C).

***Deletion of PPAR $\gamma$  does not alter timing of puberty in female mice but impairs fertility.***

Female BKO underwent vaginal opening at the same time as Flox controls (Figure 2A). Female BKO were slightly heavier (Figure 2B) and male BKO lighter (Figure 2C) than their Flox littermates during the peripubertal period (21-35 days of age) but the weight at vaginal opening was unaltered in females (Figure 2B). Fertility was assessed by mating pairs of mice over a period of 6 months. None of the breeding pairs showed a difference in the days until first litter (Figure 2D). Litter size was significantly smaller for the BKO pairs irrespective of whether the BKO was paternal or maternal suggesting that the deletion impairs both female and male fertility (Figure 2E). The BKO breeding pairs also had fewer litters than Flox/Flox breeding pairs over the course of the study (Figure 2F). Like the time until first litter, the time between litters was no different for BKO pairs (Figure 2G).

***Neuronal deletion of PPAR $\gamma$  causes hemorrhagic corpora lutea in females.***

Ovarian histology was assessed from female BKO and Flox mice. The most striking difference was the presence of hemorrhagic corpora lutea in the BKO (Figure 3A, arrows) that were not seen in the ovaries from the Flox littermates. Estrous cycles were monitored for 21 days and there was no difference between BKO and Flox mice in the number of cycles **or mean cycle length** (Figure S1A&B), or in the total days spent at each stage of the cycle (Figure 3B). Both genotypes showed a median cycle length of 5-6 days but the BKO mice tended to have more long cycles (Figure 3C) and the number of instances of prolonged diestrus/metestrus was increased (Figure 3D). Serum gonadotropins during diestrus were unchanged (Figure S1C) as were levels during afternoon (6 pm) of proestrus (Figure S1D). Plotting individual LH values clearly indicated that there were two populations of mice, those with an LH surge and those without (Figure 3E). The mean proestrus LH surge value was significantly higher in the BKO mice but the non-surge value was unaltered (Figure 3F). The BKO mice had fewer surges than the Flox mice (6/17 for BKO vs. 11/17 for Flox). Hypothalamic *Gnrh* mRNA was unaltered (Figure S1E) but pituitary *Lhb* mRNA was higher in the BKO females (Figure 3G) but *Fshb* was unchanged (Figure S1E). Diestrus estradiol and progesterone levels were unchanged (Figure S1F). We assessed the ovulatory capacity of the mice by super-ovulating and collecting oocytes. The BKO showed a significant decrease in the number of oocytes released (Figure 3H) confirming an ovulation defect.

***Diet-induced obesity impairs metabolism in female BKO mice.***

We had previously published that high-fat feeding in wild-type mice reduces serum FSH levels in males, and disrupts the LH proestrus surge in females (43). Therefore we placed female BKO mice and Flox littermates on a 60% high fat diet (HFD) for 24 weeks to test the effect of diet-induced obesity on female BKO mice. A defined 10% low fat diet (LFD) was used as a control instead of normal chow, to avoid spurious results due to undefined nutrients in the normal chow. We did not observe any difference in weight gain over the 24 weeks of high fat feeding for the two genotypes (Figure 4A). Female BKO mice gained weight at the same rate as female Flox littermates unlike their male counterparts (5). Glucose tolerance tests indicated the BKO and Flox mice become equally glucose intolerant on HFD (Figure 4B). Fasting blood glucoses were significantly higher on HFD as were fasting insulin levels (Figure 4C) and, as a result, HOMA-IR was also significantly higher on HFD. Insulin tolerance tests indicated that the BKO and Flox mice had the same insulin sensitivity as Flox mice whether on LFD or HFD (Figure 4D). Leptin levels were equivalently elevated in both BKO and Flox mice after 24 weeks of HFD (Figure 4E) but leptin sensitivity was altered. Flox mice on LFD showed the expected suppression of food intake after leptin injection, but Flox mice on HFD were completely resistant to leptin's anorexigenic effect (Figure 4F). BKO mice showed the same leptin sensitivity on LFD that was

not significantly different on HFD (Figure 4F), as we had observed for male BKO mice (5). Thus like the male BKO mice, the female BKO mice are protected from obesity-induced leptin resistance despite having equivalent body weights.

***Female BKO mice are protected from obesity-induced estrous cycle impairment.***

Female BKO mice were assessed for estrous cycles by vaginal cytology for 21 days at weeks 0, 6, 12 and 20. Representative cyclegrams for three mice from each group are shown in Figure S2. The Flox mice showed a time- and diet-dependent decrease in the number of cycles ( $p=0.04$  and  $0.014$ , respectively; Figure 5A). In contrast, the BKO mice only showed a time-dependent decrease ( $p=0.024$ ) and there was no further effect of HFD (Figure 5A). The length of the estrous cycles also varied. Cycle data were combined for the 6, 12 and 20-week time points to increase statistical power. The Flox mice showed a median cycle length of 5 days irrespective of diet but the BKO mice showed a median cycle length of 6 days on the LFD with a significant decrease in the number of 5-day cycles (Figure 5B), however the HFD group showed a median 5-day cycle like the Flox mice. The mean cycle length was also significantly longer for the BKO mice compared to the Flox mice on the LFD (Figure 5C). When the time spent in each stage was assessed, the Flox mice, but not the BKO mice, showed a time- and diet-dependent decrease in the days at proestrus ( $p=0.004$  and  $0.002$ , respectively; Figure 5D). No significant differences were found in the time in metestrus/diestrus or estrus (Figure S3A&B). Diestrus LH and FSH levels were not different in either BKO or Flox animals (Figure S3C&E). No difference was observed in FSH levels, or LH levels in mice that did not surge at proestrus (Figure S3D&F), but the surge LH values showed a time-dependent increase in Flox mice ( $p=0.014$ ) that was not seen on BKO mice (Figure 5E). We also analyzed pituitary LH release in response to GnRH and observed that pituitaries responded similarly regardless of the genotype and diet (Figure 5F).

Steroid levels were measured in serum samples taken from mice before and after HFD. Estradiol and testosterone levels were not changed by diet or genotype irrespective of the LH surge (Figure 6A) but progesterone was markedly increased ( $p=0.0001$ ) in samples from mice with LH surges (Figure 6A), confirming that a surge had occurred, and putting the mice on the HFD decreased the surge progesterone in both genotypes (Figure 6A). We assessed ovarian gene expression after sacrifice. Aromatase expression (*Cyp19a1*) was strongly suppressed by the HFD in the Flox mice but was unchanged in the BKO mice (Figure 6B). *Cyp11a1* increased in the BKO mice on HFD but *Star*, *Hsd17b1*, *Hsd3b1* and *Cyp17a1* did not change significantly.

Examination of ovarian histology showed significant differences between groups (Figure 7A). The HFD decreased the number of primary/secondary follicles in both the Flox and BKO mice (Figure 7B,  $p=0.03$ ). The number of early antral and antral follicles was no different in BKO mice or Flox mice on either diet, but the number of atretic follicles was selectively increased in the BKO mice ( $p=0.019$ ) especially on the LFD. The number of hemorrhagic follicles (Figure 7A) was significantly higher in the BKO on HFD (Figure 7C). The number of new corpora lutea (with a defined boundary) was unchanged but the number of regressing corpora lutea (no well-defined boundary) was increased in the BKO ( $p=0.01$ ) particularly on the HFD (Figure 7D) suggesting impaired luteolysis in the BKO mice.

To gain insight into potential explanations for the reproductive phenotype we measured the expression of selected inflammation and neuroendocrine genes by QPCR in hypothalamic RNA from a second cohort of male BKO mice on HFD. As expected, *Pparg* showed a genotype-dependent decrease in expression in the hypothalamus due to the knockout (Figure S4A). *Gfap* expression was unchanged indicating that loss of PPAR $\gamma$  did not cause astrocyte activation, but the JAK/STAT negative feedback regulator *Socs3* showed an HFD-dependent increase in the Flox mice but not the BKO (Figure S4A). *Gnrh1* did not change with genotype or diet (Figure S4B), whereas *Kiss1* and *Cart* showed an HFD-dependent increase in expression in both

genotypes, and *Agrp* showed an HFD-dependent increase only in the Flox mice (Figure S4B). Other neuropeptide genes implicated in reproduction including *Npy*, *Npvf* (GnIH), *Tac2* (NKB), and *Hcrt* (orexinA) did not vary with diet or genotype.

## DISCUSSION

PPAR $\gamma$  regulates a number of biological processes, including adipocyte differentiation, lipid and glucose homeostasis, and control of inflammatory responses. The effects in reproduction are less known, but PPAR $\gamma$  actions have been demonstrated in the pituitary and ovary (24;25). Loss of PPAR $\gamma$  in neurons in male mice reduces their food intake and body weight gain when fed a HFD, and abolishes leptin resistance (5). We show here that loss of neuronal PPAR $\gamma$  in female mice also prevented HFD-induced leptin resistance but, in contrast to male mice, food intake and weight gain were normal, suggesting a sexually dimorphic feeding response. If the phenotype of the male BKO mice is due to the absence of leptin resistance, then the normal feeding behavior in female BKO mice might have a number of causes. It could indicate that HFD does not induce leptin expression in the BKO mice, or that feeding is less sensitive to leptin feedback, or that different neuronal circuits control body weight or compensate for the loss of PPAR $\gamma$ . The first explanation can be discounted as leptin levels were increased equivalently in both genotypes. The second explanation is unlikely as we observed that experimental suppression of food intake by leptin injection is no different between male and female mice. The notion that different neuronal circuits control feeding is supported by the observation that male and female mice have different food anticipatory responses (44;45), different relaxin 3-dependent alcohol consumption responses (46), and different reward-related behaviors (47). At the molecular level, SOCS3 mediates hypothalamic leptin resistance due to high-fat feeding (48;49) and we observed that *Socs3* was increased in Flox mice fed a HFD, but not in the BKO mice consistent with their leptin-sensitive phenotype. Other authors have shown that PPAR $\gamma$  knockdown prevented *Socs3* transactivation induced by docosahexaenoic acid (50) and that PPAR $\gamma$  agonists were shown to induce *Socs3* in glial cells and the pancreas (51;52). Leptin signaling via the leptin receptor (LepR) and STAT activation is also required for induction of *Socs3* in the hypothalamus (53), but how PPAR $\gamma$  and STAT signaling combine to increase *Socs3* expression is not known. Knockout of *Socs3* in neurons using *Syn-cre*, the same transgene used in this report, or in whole brain using *Nestin-cre* increases sensitivity for reduction of food intake or body weight following acute leptin treatment (49). Interestingly, the whole brain knockout of *Socs3* decreases body weight gain on HFD in both males and females, and improves GTT and ITT in male mice (49). This is consistent with our previous study in male *Pparg* KO mice but inconsistent with the data presented here in females. Unfortunately the authors do not present any data on body weight gain and glucose tolerance in the *Syn-cre Soc3* knockout and interpretation of the whole brain knockout is confounded by the loss of *Socs3* in astrocytes.

At the reproductive level, female BKO mice went through puberty normally but were sub-fertile when mated over six months, with smaller litter size and frequency while on normal chow. The fertility defect was due to an ovulation defect as BKO mice released fewer oocytes when super-ovulated. The *Cre* transgene is not expressed in the ovary, so we believe that the defect is central. Female BKO had a reduced number of LH surges but the surge LH concentrations were higher. The elevated LH surge values may be due to the elevated pituitary *Lhb* mRNA expression, but the reduced frequency of surges could be related to altered hypothalamic input. We also observed that the BKO mice presented with hemorrhagic follicles and corpora lutea, and increased numbers of atretic follicles. The hemorrhage could have been



due the elevated surge LH as ovarian hyperstimulation causes vascular leakage (54). There also appeared to be a defect in luteolysis in the BKO with the persistence of regressing corpora lutea. When placed on a HFD, female Flox mice had a reduced number of estrous cycles and a reduction in the time spent in proestrus, but female BKO mice did not show this impairment suggesting that the effect was centrally mediated and required functional PPAR $\gamma$  in neurons. Obesity can also alter ovarian function (55). Indeed, the dramatic reduction of aromatase (*Cyp19a1*) expression in obese mice is consistent with the elevated leptin, as leptin induces *Cart* expression in granulosa cells to lower *Cyp19a1* expression (56). Interestingly, aromatase down-regulation was not seen in the BKO but we do not know whether this reflected a difference in leptin signaling in the ovary or whether the effect was centrally mediated. At the pituitary, we did not see a change in sensitivity to a bolus of GnRH, although it has been reported that obesity and/or hyperinsulinemia increase pituitary gonadotrope sensitivity to GnRH (43;57).

At the hypothalamic level, the *LepR* is not expressed in *Gnrh1* neurons but is co-expressed in a subset of *Kiss1* neurons that become leptin responsive after puberty (58). Loss of *LepR* in mature neurons prevents puberty and causes infertility, but loss in *Kiss1* neurons alone does not (59). Leptin stimulates *Kiss1* expression, so the effect of HFD on *Kiss1* expression in our study may be mediated by the increased leptin levels in the obese animals. The observation that *Kiss1* was elevated in both Flox and BKO mice also suggests that the *Kiss1* neuron itself is not leptin resistant. Leptin normally suppresses *AgRP* neuronal activity and gene expression (19), but diet-induced obesity causes leptin resistance and persistent activation of these neurons (60), which is consistent with the observed increase in *AgRP* expression in obesity. Furthermore, ablation of *AgRP* neurons in *LepR*-deficient mice restores fertility indicating a central role for *AgRP* in reproductive suppression due to leptin deficiency (23). Interestingly, the only hypothalamic gene to show differential expression in the BKO mice was *AgRP*. The lack of induction of *AgRP* by HFD in the BKO mice suggests that PPAR $\gamma$  mediates leptin resistance in *AgRP* neurons. A conditional knockout of the *LepR* in *AgRP* neurons causes increased adiposity, but neither a detailed analysis of reproductive function nor a study of the effect of HFD was performed (61;62). In support of our model, intraperitoneal administration of the PPAR $\gamma$  agonist rosiglitazone increases *AgRP* mRNA in the ARC in hamsters and mice (63). Furthermore, *AgRP* neurons are more responsive to low levels of leptin, and are more prone to SOCS3 induction and leptin resistance (64). GnRH neuron activity rather than gene expression may be restrained by PPAR $\gamma$  through *AgRP* induction as *AgRP* fibers form synapses on GnRH neurons in mice (65) and infusion of *AgRP* suppresses pulsatile LH release in ovariectomized monkeys (66).

In conclusion, the results presented here show that neuronal PPAR $\gamma$  was necessary for normal LH surges and female fertility, but was also involved in the adverse effects of diet-induced obesity on estrous cycles by creating leptin resistance in *AgRP* neurons potentially through induction of the repressor gene *Socs3*. Our data are consistent with clinical observations as TZD therapy in women with PCOS decreases serum LH and increases ovulation rate (31;32). Further detailed studies using genetic deletions in specific neuronal populations will be necessary to dissect the individual contributions of PPAR $\gamma$ , SOCS3 and *AgRP* to leptin resistance and reproductive function in cases of lipid excess and obesity.

#### ACKNOWLEDGEMENTS:

We would like to acknowledge the assistance of the Histology Core at the Moores' Cancer Center, and the Genomics Core at the Sanford Consortium for Regenerative Medicine. This work is funded in part by NIH grants to N.J.G.W. (HD012303, CA155435, CA023100, CA196853) and J.M.O. (DK033651, DK074868, DK063491, DK09062), and a VA Merit Review award to N.J.G.W. (I01BX000130).

Corresponding author: Nicholas Webster, PhD, Department of Medicine – 0673,  
University of California, San Diego, 9500 Gilman Drive, La Jolla, CA 92093, Email:  
nwebster@ucsd.edu

## REFERENCES

1. Semple RK, Chatterjee VK, O'Rahilly S 2006 PPAR gamma and human metabolic disease. *J Clin Invest* 116:581-589
2. Lehrke M, Lazar MA 2005 The many faces of PPARgamma. *Cell* 123:993-999
3. Shimizu H, Tsuchiya T, Sato N, Shimomura Y, Kobayashi I, Mori M 1998 Troglitazone reduces plasma leptin concentration but increases hunger in NIDDM patients. *Diabetes Care* 21:1470-1474
4. Sarruf DA, Yu F, Nguyen HT, Williams DL, Printz RL, Niswender KD, Schwartz MW 2009 Expression of peroxisome proliferator-activated receptor-gamma in key neuronal subsets regulating glucose metabolism and energy homeostasis. *Endocrinology* 150:707-712
5. Lu M, Sarruf DA, Talukdar S, Sharma S, Li P, Bandyopadhyay G, Nalbandian S, Fan W, Gayen JR, Mahata SK, Webster NJ, Schwartz MW, Olefsky JM 2011 Brain PPAR-gamma promotes obesity and is required for the insulin-sensitizing effect of thiazolidinediones. *Nat Med* 17:618-622
6. Keen-Rhinehart E, Ondek K, Schneider JE 2013 Neuroendocrine regulation of appetitive ingestive behavior. *Front Neurosci* 7:213
7. Sobrino CC, Perianes CA, Puebla JL, Barrios V, Arilla FE 2014 Peptides and food intake. *Front Endocrinol (Lausanne)* 5:58
8. Castro AV, Kolka CM, Kim SP, Bergman RN 2014 Obesity, insulin resistance and comorbidities? Mechanisms of association. *Arq Bras Endocrinol Metabol* 58:600-609
9. Crujeiras AB, Carreira MC, Cabia B, Andrade S, Amil M, Casanueva FF 2015 Leptin resistance in obesity: An epigenetic landscape. *Life Sci*
10. Wellen KE, Hotamisligil GS 2005 Inflammation, stress, and diabetes. *J Clin Invest* 115:1111-1119
11. Valdearcos M, Xu AW, Koliwad SK 2015 Hypothalamic inflammation in the control of metabolic function. *Annu Rev Physiol* 77:131-160
12. Herbison AE 2006 Physiology of the GnRH neuronal network. In: Neill JD, ed. *Knobil and Neill's physiology of reproduction*. Third Edition ed. San Diego: Elsevier, Academic Press; 1415-1482
13. Pawson AJ, McNeilly AS 2005 The pituitary effects of GnRH. *Anim Reprod Sci* 88:75-94
14. Oakley AE, Clifton DK, Steiner RA 2009 Kisspeptin signaling in the brain. *Endocr Rev* 30:713-743
15. Kauffman AS 2010 Coming of age in the kisspeptin era: sex differences, development, and puberty. *Mol Cell Endocrinol* 324:51-63
16. Semaan SJ, Tolson KP, Kauffman AS 2013 The development of kisspeptin circuits in the Mammalian brain. *Adv Exp Med Biol* 784:221-252
17. Sanz E, Quintana A, Deem JD, Steiner RA, Palmiter RD, McKnight GS 2015 Fertility-regulating Kiss1 neurons arise from hypothalamic POMC-expressing progenitors. *J Neurosci* 35:5549-5556
18. Nestor CC, Qiu J, Padilla SL, Zhang C, Bosch MA, Fan W, Aicher SA, Palmiter RD, Ronnekleiv OK, Kelly MJ 2016 Optogenetic Stimulation of Arcuate Nucleus Kiss1 Neurons Reveals a Steroid-Dependent Glutamatergic Input to POMC and AgRP Neurons in Male Mice. *Mol Endocrinol* 30:630-644

19. Klenke U, Constantin S, Wray S 2010 Neuropeptide Y directly inhibits neuronal activity in a subpopulation of gonadotropin-releasing hormone-1 neurons via Y1 receptors. *Endocrinology* 151:2736-2746
20. True C, Verma S, Grove KL, Smith MS 2013 Cocaine- and amphetamine-regulated transcript is a potent stimulator of GnRH and kisspeptin cells and may contribute to negative energy balance-induced reproductive inhibition in females. *Endocrinology* 154:2821-2832
21. Ratra DV, Elias CF 2014 Chemical identity of hypothalamic neurons engaged by leptin in reproductive control. *J Chem Neuroanat* 61-62:233-238
22. Bellefontaine N, Elias CF 2014 Minireview: Metabolic control of the reproductive physiology: insights from genetic mouse models. *Horm Behav* 66:7-14
23. Sheffer-Babila S, Sun Y, Israel DD, Liu SM, Neal-Perry G, Chua SC, Jr. 2013 Agouti-related peptide plays a critical role in leptin's effects on female puberty and reproduction. *Am J Physiol Endocrinol Metab* 305:E1512-E1520
24. Sharma S, Sharma PM, Mistry DS, Chang RJ, Olefsky JM, Mellon PL, Webster NJ 2011 PPAR $\gamma$  regulates gonadotropin-releasing hormone signaling in L $\beta$ T2 cells in vitro and pituitary gonadotroph function in vivo in mice. *Biol Reprod* 84:466-475
25. Kim J, Sato M, Li Q, Lydon JP, DeMayo FJ, Bagchi IC, Bagchi MK 2008 Peroxisome proliferator-activated receptor gamma is a target of progesterone regulation in the preovulatory follicles and controls ovulation in mice. *Mol Cell Biol* 28:1770-1782
26. Korhonen S, Heinonen S, Hiltunen M, Helisalmi S, Hippelainen M, Koivunen R, Tapanainen JS, Laakso M 2003 Polymorphism in the peroxisome proliferator-activated receptor-gamma gene in women with polycystic ovary syndrome. *Hum Reprod* 18:540-543
27. Orio F, Jr., Matarese G, Di BS, Palomba S, Labella D, Sanna V, Savastano S, Zullo F, Colao A, Lombardi G 2003 Exon 6 and 2 peroxisome proliferator-activated receptor-gamma polymorphisms in polycystic ovary syndrome. *J Clin Endocrinol Metab* 88:5887-5892
28. Lujan ME, Chizen DR, Pierson RA 2008 Diagnostic criteria for polycystic ovary syndrome: pitfalls and controversies. *J Obstet Gynaecol Can* 30:671-679
29. Dereli D, Dereli T, Bayraktar F, Ozgen AG, Yilmaz C 2005 Endocrine and metabolic effects of rosiglitazone in non-obese women with polycystic ovary disease. *Endocr J* 52:299-308
30. Khan KA, Stas S, Kurukulasuriya LR 2006 Polycystic ovarian syndrome. *J Cardiometab Syndr* 1:125-130
31. Azziz R, Ehrmann D, Legro RS, Whitcomb RW, Hanley R, Fereshetian AG, O'Keefe M, Ghazzi MN 2001 Troglitazone improves ovulation and hirsutism in the polycystic ovary syndrome: a multicenter, double blind, placebo-controlled trial. *J Clin Endocrinol Metab* 86:1626-1632
32. Mehta RV, Patel KS, Coffler MS, Dahan MH, Yoo RY, Archer JS, Malcom PJ, Chang RJ 2005 Luteinizing hormone secretion is not influenced by insulin infusion in women with polycystic ovary syndrome despite improved insulin sensitivity during pioglitazone treatment. *J Clin Endocrinol Metab* 90:2136-2141
33. Sharma S, Sharma PM, Mistry DS, Chang RJ, Olefsky JM, Mellon PL, Webster N 2010 PPAR $\gamma$  Regulates Gonadotropin-Releasing Hormone Signaling in L $\beta$ T2 Cells In Vitro and Pituitary Gonadotroph Function In Vivo in Mice. *Biol Reprod*
34. He W, Barak Y, Hevener A, Olson P, Liao D, Le J, Nelson M, Ong E, Olefsky JM, Evans RM 2003 Adipose-specific peroxisome proliferator-activated receptor gamma knockout causes insulin resistance in fat and liver but not in muscle. *Proc Natl Acad Sci U S A* 100:15712-15717

35. Hevener AL, He W, Barak Y, Le J, Bandyopadhyay G, Olson P, Wilkes J, Evans RM, Olefsky J 2003 Muscle-specific Pparg deletion causes insulin resistance. *Nat Med* 9:1491-1497
36. Zhu Y, Romero MI, Ghosh P, Ye Z, Charnay P, Rushing EJ, Marth JD, Parada LF 2001 Ablation of NF1 function in neurons induces abnormal development of cerebral cortex and reactive gliosis in the brain. *Genes Dev* 15:859-876
37. Rempe D, Vangeison G, Hamilton J, Li Y, Jepson M, Federoff HJ 2006 Synapsin I Cre transgene expression in male mice produces germline recombination in progeny. *Genesis* 44:44-49
38. Yamanaka T, Tosaki A, Kurosawa M, Akimoto K, Hirose T, Ohno S, Hattori N, Nukina N 2013 Loss of aPKC $\lambda$  in differentiated neurons disrupts the polarity complex but does not induce obvious neuronal loss or disorientation in mouse brains. *PLoS One* 8:e84036
39. Ren H, Plum-Morschel L, Gutierrez-Juarez R, Lu TY, Kim-Muller JY, Heinrich G, Wardlaw SL, Silver R, Accili D 2013 Blunted refeeding response and increased locomotor activity in mice lacking FoxO1 in synapsin-Cre-expressing neurons. *Diabetes* 62:3373-3383
40. He XP, Kotloski R, Nef S, Luikart BW, Parada LF, McNamara JO 2004 Conditional deletion of TrkB but not BDNF prevents epileptogenesis in the kindling model. *Neuron* 43:31-42
41. Pelusi C, Ikeda Y, Zubair M, Parker KL 2008 Impaired follicle development and infertility in female mice lacking steroidogenic factor 1 in ovarian granulosa cells. *Biol Reprod* 79:1074-1083
42. Myers M, Britt KL, Wreford NG, Ebling FJ, Kerr JB 2004 Methods for quantifying follicular numbers within the mouse ovary. *Reproduction* 127:569-580
43. Sharma S, Morinaga H, Hwang V, Fan W, Fernandez MO, Varki N, Olefsky JM, Webster NJ 2013 Free fatty acids induce Lhb mRNA but suppress Fshb mRNA in pituitary LbetaT2 gonadotropes and diet-induced obesity reduces FSH levels in male mice and disrupts the proestrous LH/FSH surge in female mice. *Endocrinology* 154:2188-2199
44. Michalik M, Steele AD, Mistlberger RE 2015 A sex difference in circadian food-anticipatory rhythms in mice: Interaction with dopamine D1 receptor knockout. *Behav Neurosci* 129:351-360
45. Li Z, Wang Y, Sun KK, Wang K, Sun ZS, Zhao M, Wang J 2015 Sex-related difference in food-anticipatory activity of mice. *Horm Behav* 70:38-46
46. Shirahase T, Aoki M, Watanabe R, Watanabe Y, Tanaka M 2016 Increased alcohol consumption in relaxin-3 deficient male mice. *Neurosci Lett* 612:155-160
47. Seu E, Groman SM, Arnold AP, Jentsch JD 2014 Sex chromosome complement influences operant responding for a palatable food in mice. *Genes Brain Behav* 13:527-534
48. Liu ZJ, Bian J, Zhao YL, Zhang X, Zou N, Li D 2011 Lentiviral vector-mediated knockdown of SOCS3 in the hypothalamus protects against the development of diet-induced obesity in rats. *Diabetes Obes Metab* 13:885-892
49. Mori H, Hanada R, Hanada T, Aki D, Mashima R, Nishinakamura H, Torisu T, Chien KR, Yasukawa H, Yoshimura A 2004 Socs3 deficiency in the brain elevates leptin sensitivity and confers resistance to diet-induced obesity. *Nat Med* 10:739-743
50. Berger H, Vegran F, Chikh M, Gilardi F, Ladoire S, Bugaut H, Mignot G, Chalmin F, Bruchard M, Derangere V, Chevriaux A, Rebe C, Ryffel B, Pot C, Hichami A, Desvergne B, Ghiringhelli F, Apetoh L 2013 SOCS3 transactivation by PPAR $\gamma$  prevents IL-17-driven cancer growth. *Cancer Res* 73:3578-3590

51. Park EJ, Park SY, Joe EH, Jou I 2003 15d-PGJ2 and rosiglitazone suppress Janus kinase-STAT inflammatory signaling through induction of suppressor of cytokine signaling 1 (SOCS1) and SOCS3 in glia. *J Biol Chem* 278:14747-14752
52. Yu JH, Kim KH, Kim H 2008 SOCS 3 and PPAR-gamma ligands inhibit the expression of IL-6 and TGF-beta1 by regulating JAK2/STAT3 signaling in pancreas. *Int J Biochem Cell Biol* 40:677-688
53. Pedroso JA, Buonfiglio DC, Cardinali LI, Furigo IC, Ramos-Lobo AM, Tirapegui J, Elias CF, Donato J, Jr. 2014 Inactivation of SOCS3 in leptin receptor-expressing cells protects mice from diet-induced insulin resistance but does not prevent obesity. *Mol Metab* 3:608-618
54. Delbaere A, Smits G, De LA, Costagliola S, Vassart G 2005 Understanding ovarian hyperstimulation syndrome. *Endocrine* 26:285-290
55. Huang-Doran I, Franks S 2016 Genetic Rodent Models of Obesity-Associated Ovarian Dysfunction and Subfertility: Insights into Polycystic Ovary Syndrome. *Front Endocrinol (Lausanne)* 7:53
56. Ma X, Hayes E, Prizant H, Srivastava RK, Hammes SR, Sen A 2016 Leptin-Induced CART (Cocaine- and Amphetamine-Regulated Transcript) Is a Novel Intraovarian Mediator of Obesity-Related Infertility in Females. *Endocrinology* 157:1248-1257
57. Brothers KJ, Wu S, DiVall SA, Messmer MR, Kahn CR, Miller RS, Radovick S, Wondisford FE, Wolfe A 2010 Rescue of obesity-induced infertility in female mice due to a pituitary-specific knockout of the insulin receptor. *Cell Metab* 12:295-305
58. Cravo RM, Frazao R, Perello M, Osborne-Lawrence S, Williams KW, Zigman JM, Vianna C, Elias CF 2013 Leptin signaling in Kiss1 neurons arises after pubertal development. *PLoS One* 8:e58698
59. Donato J, Jr., Cravo RM, Frazao R, Gautron L, Scott MM, Lachey J, Castro IA, Margatho LO, Lee S, Lee C, Richardson JA, Friedman J, Chua S Jr, Coppari R, Zigman JM, Elmquist JK, Elias CF 2011 Leptin's effect on puberty in mice is relayed by the ventral premammillary nucleus and does not require signaling in Kiss1 neurons. *J Clin Invest* 121:355-368
60. Baver SB, Hope K, Guyot S, Bjorbaek C, Kaczorowski C, O'Connell KM 2014 Leptin modulates the intrinsic excitability of AgRP/NPY neurons in the arcuate nucleus of the hypothalamus. *J Neurosci* 34:5486-5496
61. van de Wall E, Leshan R, Xu AW, Balthasar N, Coppari R, Liu SM, Jo YH, MacKenzie RG, Allison DB, Dun NJ, Elmquist J, Lowell BB, Barsh GS, de LC, Myers MG, Jr., Schwartz GJ, Chua SC, Jr. 2008 Collective and individual functions of leptin receptor modulated neurons controlling metabolism and ingestion. *Endocrinology* 149:1773-1785
62. Luo N, Marcellin G, Liu SM, Schwartz G, Chua S Jr 2011 Neuropeptide Y and agouti-related peptide mediate complementary functions of hyperphagia and reduced energy expenditure in leptin receptor deficiency. *Endocrinology* 152:883-889
63. Garretson JT, Teubner BJ, Grove KL, Vazdarjanova A, Ryu V, Bartness TJ 2015 Peroxisome proliferator-activated receptor gamma controls ingestive behavior, agouti-related protein, and neuropeptide Y mRNA in the arcuate hypothalamus. *J Neurosci* 35:4571-4581
64. Olofsson LE, Unger EK, Cheung CC, Xu AW 2013 Modulation of AgRP-neuronal function by SOCS3 as an initiating event in diet-induced hypothalamic leptin resistance. *Proc Natl Acad Sci U S A* 110:E697-E706
65. Turi GF, Liposits Z, Moenter SM, Fekete C, Hrabovszky E 2003 Origin of neuropeptide Y-containing afferents to gonadotropin-releasing hormone neurons in male mice. *Endocrinology* 144:4967-4974

66. Vulliamoz NR, Xiao E, Xia-Zhang L, Wardlaw SL, Ferin M 2005 Central infusion of agouti-related peptide suppresses pulsatile luteinizing hormone release in the ovariectomized rhesus monkey. *Endocrinology* 146:784-789

**Figure 1: PPAR $\gamma$  gene targeting.** (A) DNA was extracted from the indicated tissues and PCR analysis was carried out for recombination. (B) Total RNA was isolated from the indicated tissues of WT (white) and BKO (green) mice. PPAR $\gamma$  mRNA levels were measured by Q-PCR analysis. Data shown are the fold induction of gene expression normalized with housekeeping gene and expressed as mean  $\pm$ SEM. Asterisk indicates statistical significance, \* $p$ <0.05. (C) Immunohistochemical analysis of coronal sections of brain from WT and BKO mice. Arrows indicate nuclear (blue) and PPAR $\gamma$  (black) staining.

**Figure 2: Puberty and fertility assessment in BKO mice.** (A) Percentage of mice undergoing vaginal opening over time. Inset shows day of vaginal opening (mean  $\pm$ SEM). Flox mice are shown in white, BKO mice in green. (B) Female weights during puberty. Inset shows weight at vaginal opening (mean  $\pm$ SEM). Asterisks indicate statistical significance for BKO vs Flox mice, \* $p$ <0.05, \*\* $p$ <0.01 by 2-way ANOVA. (C) Male body weights after weaning (mean  $\pm$ SEM). (D) Six week old BKO and Flox mice were paired in different combinations and bred over a period of six months. Average days before the first litter was born to the breeding pair (mean  $\pm$ SEM). Flox/Flox breeding is shown in white, BKO/BKO breeding in green and the mixed Flox/BKO breeding in red and blue. (E) Average number of pups born to the indicated breeding pairs (mean  $\pm$ SEM). Asterisk indicates statistical significance vs. Flox:Flox, \*\* $p$ <0.01 by ANOVA. (F) Number of litters over 6 months (mean  $\pm$ SEM). Asterisk indicates statistical significance vs Flox:Flox, \* $p$ <0.05 by ANOVA. (G) Days between litters over 6 months (mean  $\pm$ SEM).

**Figure 3: Histological analysis of ovaries, estrous cycles and hormone levels from adult Flox and BKO mice.** (A) H&E stained sections of ovaries from 13-week old mice. Arrows indicate hemorrhagic corpora lutea. (B) Percentage of days in metestrus/diestrus, estrus or proestrus (mean  $\pm$ SEM). Flox mice are shown in white, BKO mice in green. (C) Distribution of estrous cycle length in Flox and BKO mice. Cycle length was defined as the end of estrus to the end of the next estrus. (D) Number of cycles with prolonged diestrus. A prolonged diestrus stage was defined as greater than 3 or 4 days of metestrus or diestrus (mean  $\pm$ SEM). BKO mice showed a greater number of prolonged cycles (genotype effect  $p$ =0.005 by 2-way ANOVA). (E) Individual plasma LH levels measured at 6 pm on the day of proestrus. (F) Plasma LH values separated into mice that showed an LH surge and those that did not. Individual values are shown along with mean  $\pm$ SEM. (G) Pituitary *Lhb* mRNA expression by QPCR. (H) Number of oocytes released following induction of ovulation. Asterisks indicate statistical significance as indicated by t-test or post-hoc testing following 2-way ANOVA, \* $p$ <0.05.

**Figure 4. Body weights and metabolic characterization of adult female BKO mice on HFD.** Mice were placed on a 60% high-fat diet (HFD) or a matched 10% low-fat diet (LFD) for 24 weeks. (A) Body weight over time on diets (mean  $\pm$ SEM). The Flox mice on LFD group is shown in white, the Flox mice on HFD group is shown in red, the BKO mice on LFD group is shown in green, and the BKO mice on HFD group is shown in blue. Flox mice are shown by circles, BKO mice by squares. Body weights on LFD or HFD show a time effect ( $p$ <0.0001) but no genotype effect or interaction by repeated measures 2-way ANOVA. (B) Intraperitoneal glucose tolerance tests (1g/kg body weight) performed on mice after 17 weeks on diets. Tail

vein glucose was measured over 120 min (mean  $\pm$ SEM), \*\*\*\* $p < 0.0001$  for diet effect. (C) Fasting blood glucose (FBG), fasting insulin (FI) and HOMA-IR measurements for Flox and BKO mice (mean  $\pm$ SEM). FBG, FI and HOMA-IR showed significant diet effects ( $p = 0.005$ ,  $0.028$  and  $0.025$ , respectively) by 2-way ANOVA. (D) Insulin tolerance tests performed on mice after 20 weeks on diets. Mice on LFD received 0.4 IU/kg insulin, whereas those on HFD received 0.75 IU/kg due to their insulin resistance. Tail vein glucose was measured over 120 min (mean  $\pm$ SEM). (E) Fasted leptin levels in Flox and BKO mice after 20 weeks on LFD or HFD (mean  $\pm$ SEM). Leptin showed a very significant diet effect ( $p < 0.0001$ ). (F) Leptin suppression of food intake. Mice received daily injections of leptin for 2 days then injections of saline for 2 days and food intake was measured (mean  $\pm$ SEM). Suppression of food intake showed a significant diet effect ( $p = 0.0041$ ) primarily in the Flox mice. Asterisks indicate statistical significance as indicated, \* $p < 0.05$ , \*\*  $p < 0.01$ , \*\*\* $p < 0.001$ , \*\*\*\* $p < 0.0001$ .

**Figure 5: Estrous cycles over time on HFD diet.** Estrous cycles were monitored by vaginal cytology for 21 days at 6, 12 and 20 weeks on diets. (A) Number of cycles over time on diets. A cycle was defined as a day of diestrus, followed by a day of proestrus, then a day of estrus. The Flox mice on LFD group is shown in white, the Flox mice on HFD group is shown in red, the BKO mice on LFD group is shown in green, and the BKO mice on HFD group is shown in blue. Data are shown as mean  $\pm$ SEM. Flox mice showed a significant time and diet effect by 2-way ANOVA, but BKO did not show a difference with diet. (B) Distribution of cycle length for Flox and BKO on LFD and HFD. Cycle length was defined as the end of estrus to the end of the next estrus. Data from 6, 12 and 20 weeks was combined. (C) Mean cycle length (mean  $\pm$ SEM). Cycle length showed a genotype effect ( $p = 0.01$ ) and a significant interaction of genotype and diet ( $p = 0.0004$ ) by 2-way ANOVA. (D) Percentage of days in proestrus. Data are shown as mean  $\pm$ SEM. The Flox mice showed significant time and diet effects ( $p = 0.004$  and  $0.002$ , respectively). (E) Surge LH values during the afternoon (6 pm) of proestrus. The Flox mice showed significant time effect ( $p = 0.014$ ). (F) GnRH stimulated LH release. Mice received GnRH (1  $\mu$ g/kg) in the morning after 18 weeks on diets. Tail vein blood was taken before and 10 min after GnRH injection (GnRH, striped bars). Data are shown as mean  $\pm$ SEM. LH values showed a very significant GnRH effect ( $p < 0.0001$ ) but no differences between groups. Asterisks indicate statistical significance by post-hoc testing following 2-way ANOVA, \* =  $p < 0.05$ , \*\*\* $p < 0.001$ .

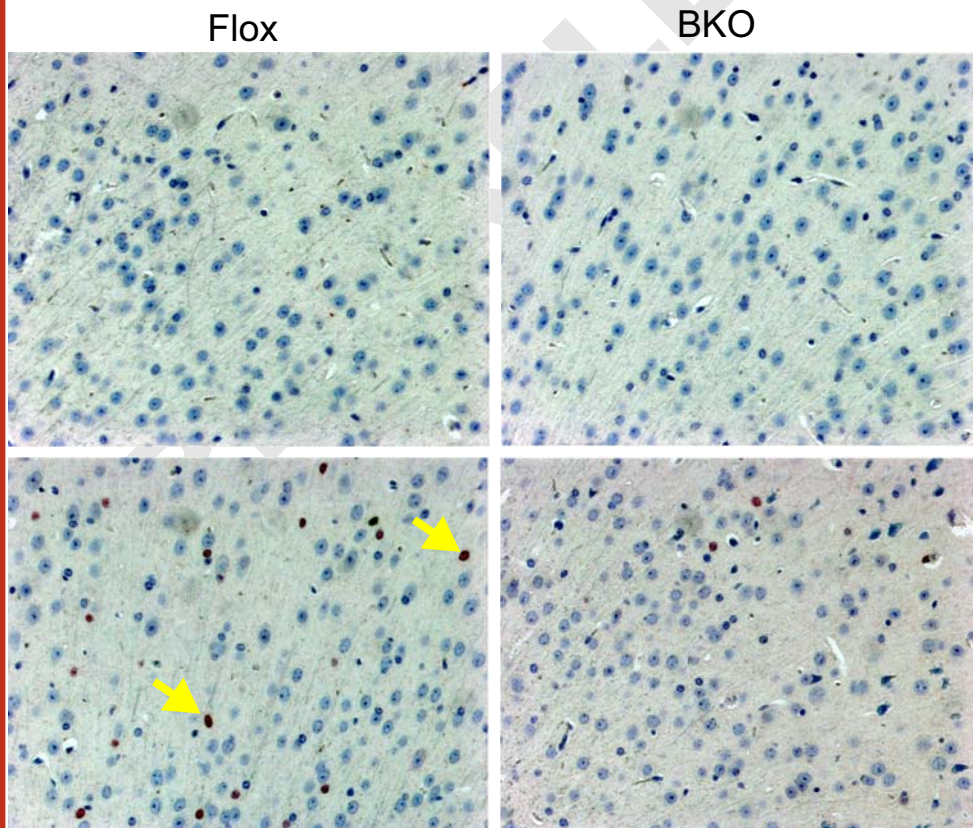
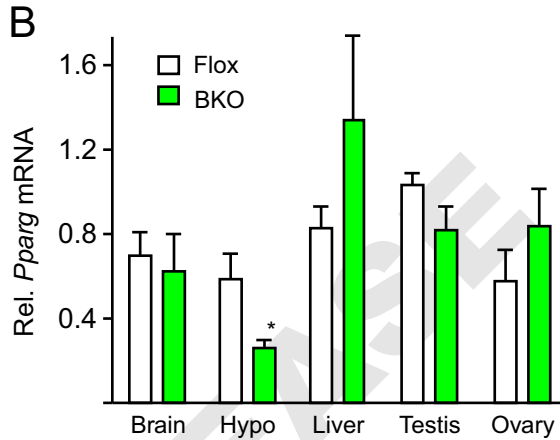
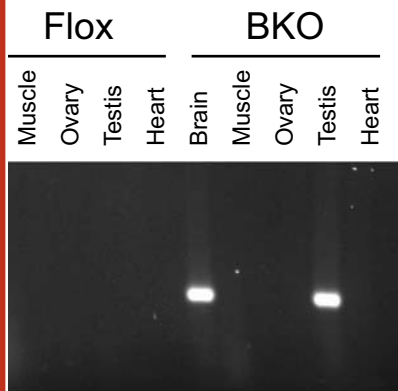
**Figure 6: Steroid levels and ovarian gene expression.** (A) Plasma steroid levels during proestrus for mice with or without LH surges, before or after HFD. Data are shown as mean  $\pm$ SEM. Estradiol and progesterone showed significant surge increases ( $p = 0.0027$  and  $< 0.0001$ , respectively) by 2-way ANOVA, and the surge progesterone values showed a HFD-dependent decrease ( $p = 0.015$ ). (B) Ovarian expression of steroid biosynthetic genes *Cyp19a1*, *Hsd17b1*, *Star*, *Hsd3b1*, *Cyp11a1* and *Cyp17a1* by QPCR. The Flox mice on LFD group is shown in white, the Flox mice on HFD group is shown in red, the BKO mice on LFD group is shown in green, and the BKO mice on HFD group is shown in blue. *Cyp19a1* expression showed a significant interaction of diet and genotype ( $p = 0.0089$ ) by 2-way ANOVA. Asterisks indicate statistical significance by post-hoc testing after 2-way ANOVA as indicated, \* $p < 0.05$ .

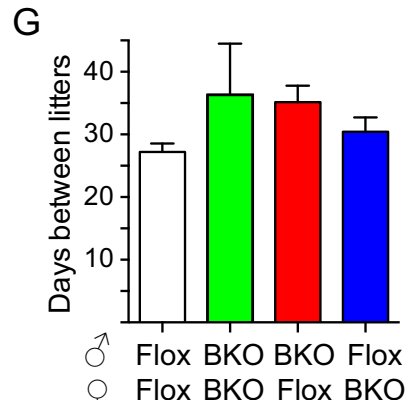
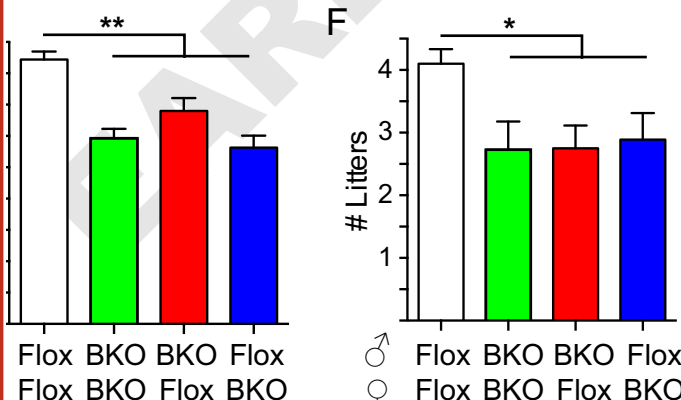
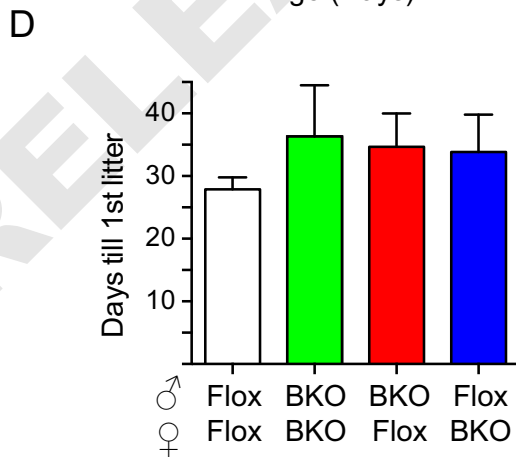
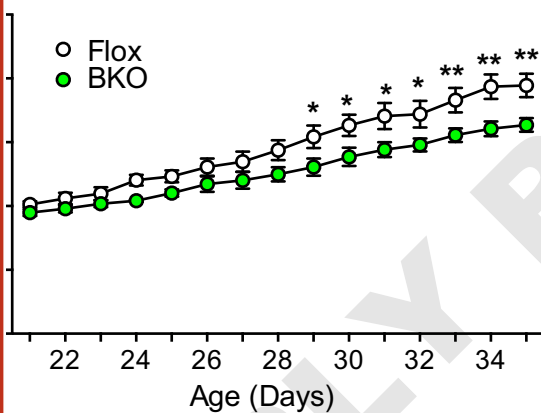
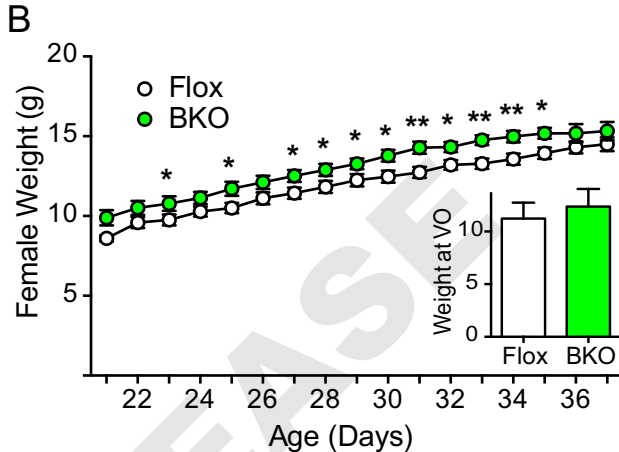
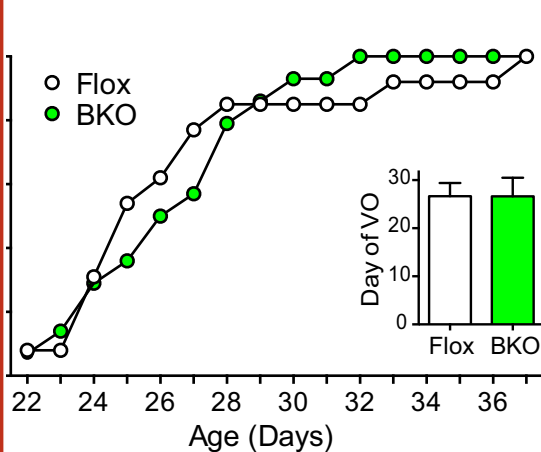
**Figure 7: Ovarian histology for mice on HFD.** Mice were sacrificed after 24 weeks on diets. (A) Representative H&E stained sections of ovaries from Flox and BKO mice on LFD and HFD. Yellow arrow indicates hemorrhagic follicle. (B) Number of staged follicles per 3 ovary sections (mean  $\pm$ SEM). Primary/secondary follicle number showed a diet effect ( $p = 0.03$ ) and atretic

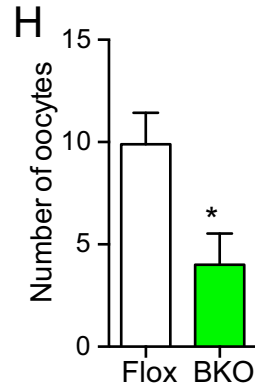
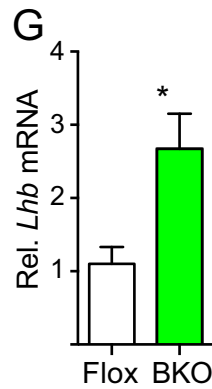
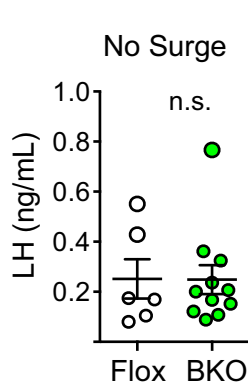
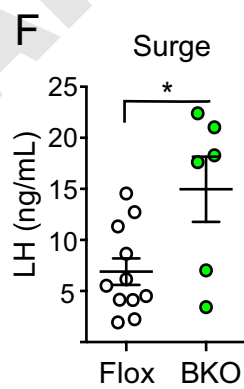
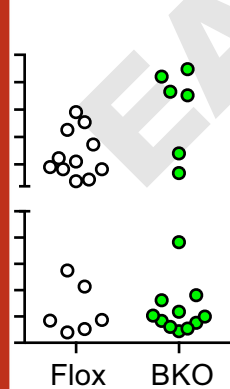
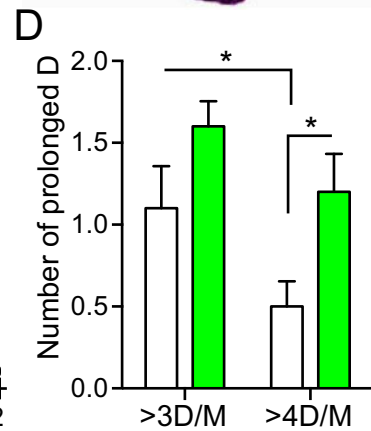
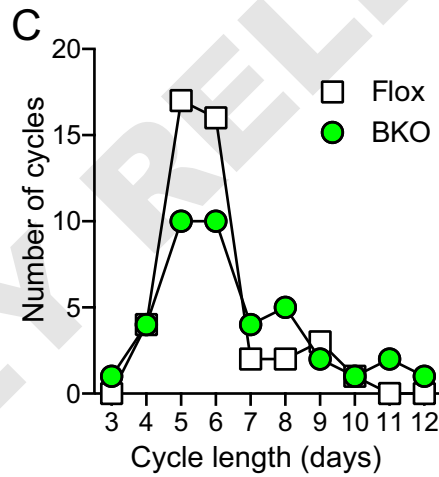
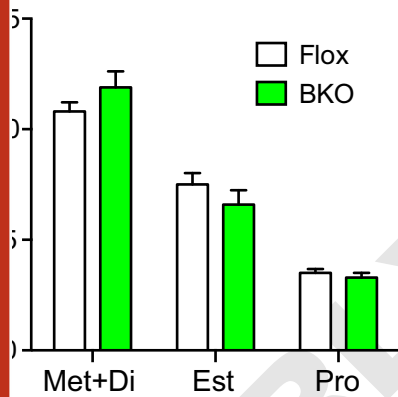
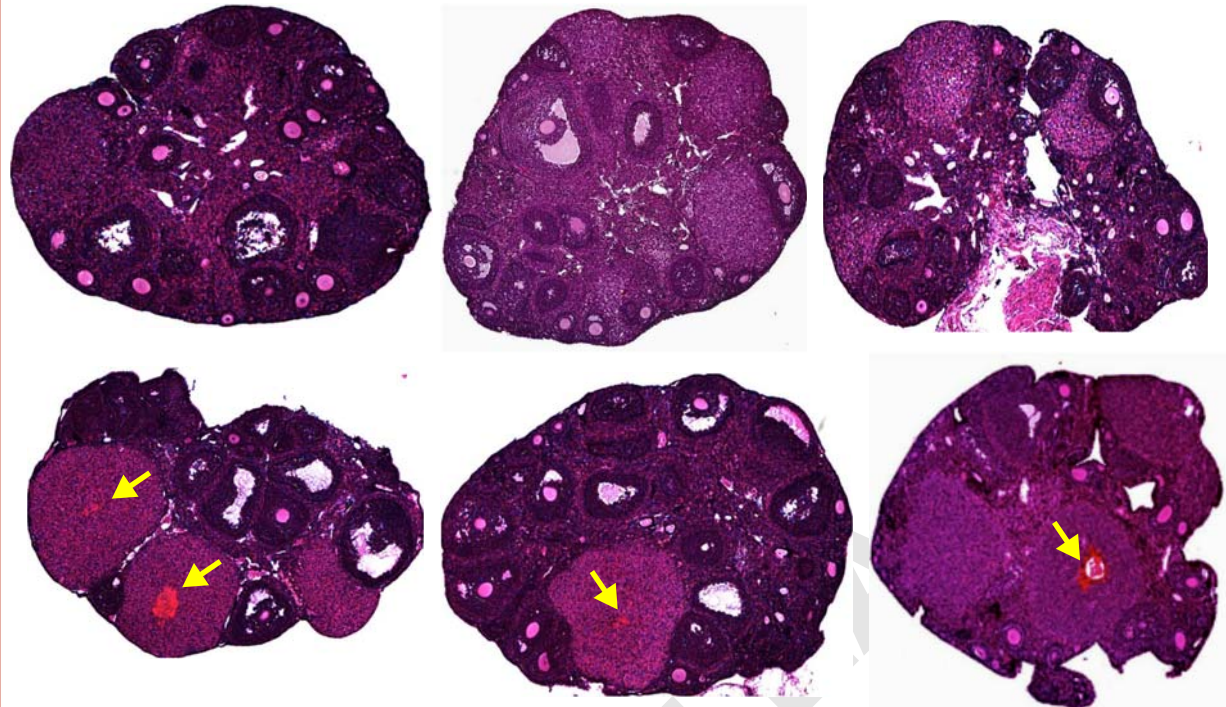
follicle number showed a genotype effect ( $p=0.013$ ) by 2-Way ANOVA. **(C)** Number of hemorrhagic follicles per 3 ovary sections (mean  $\pm$ SEM). Diet effect  $p=0.005$ , genotype effect  $p=0.02$ , interaction  $p=0.02$  by 2-Way ANOVA. **(D)** Number of corpora lutea per 3 ovary sections (mean  $\pm$ SEM). Genotype effect  $p=0.01$  by 2-way ANOVA, ND: none detected. The Flox mice on LFD group is shown in white, the Flox mice on HFD group is shown in red, the BKO mice on LFD group is shown in green, and the BKO mice on HFD group is shown in blue. Asterisks indicate statistical significance by post-hoc testing after 2-way ANOVA as indicated, \* $p<0.05$ , \*\* $p<0.01$ , \*\*\* $p<0.001$ .

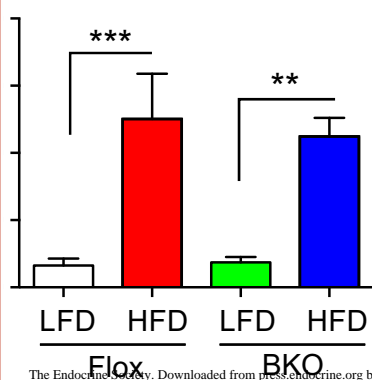
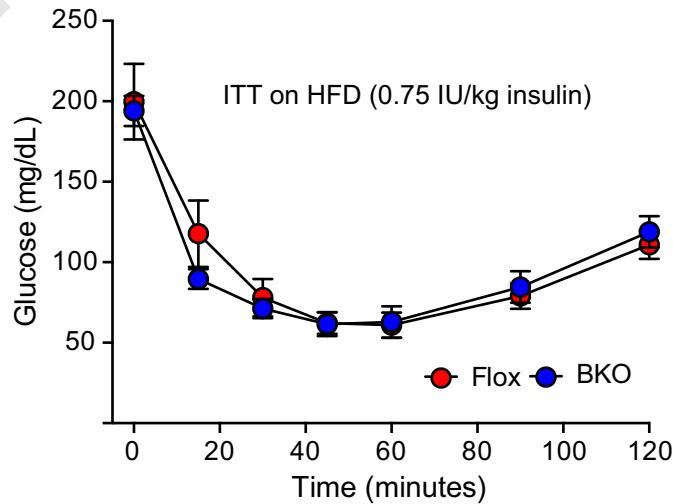
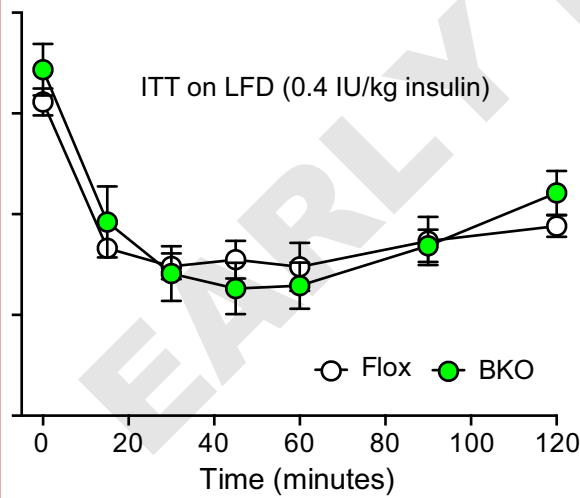
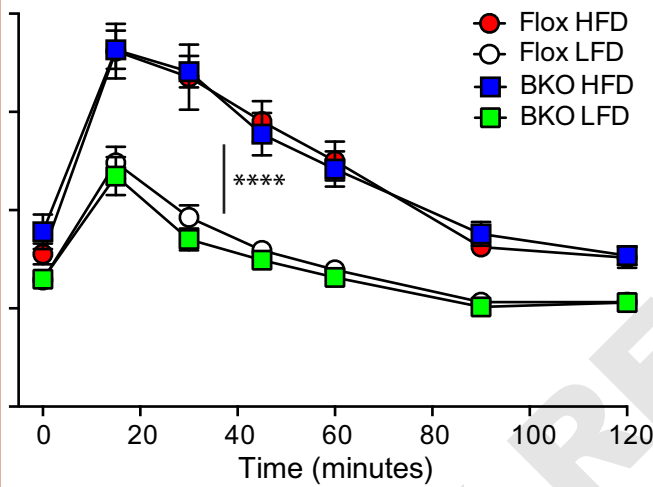
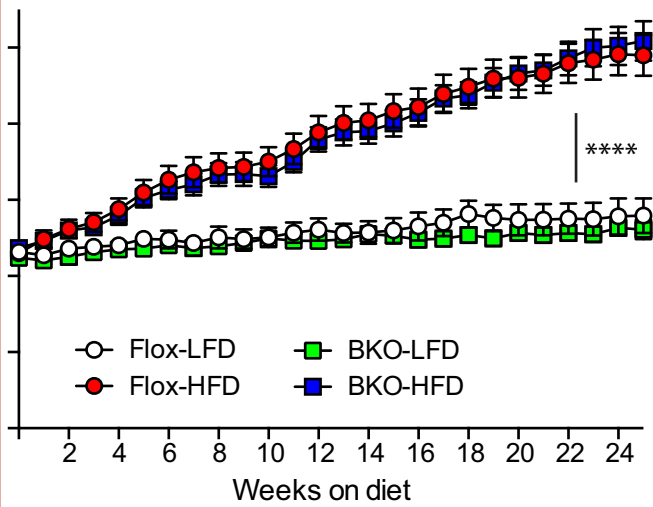
EARLY RELEASE



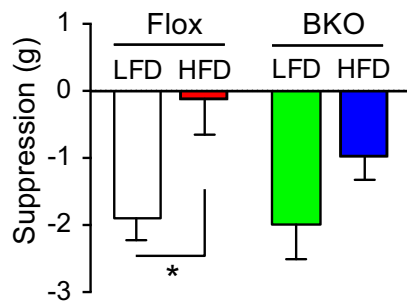




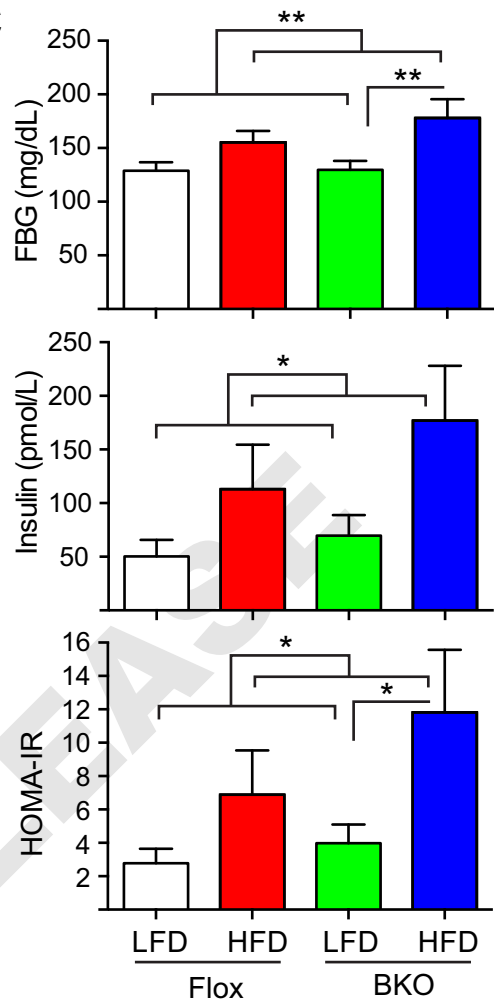


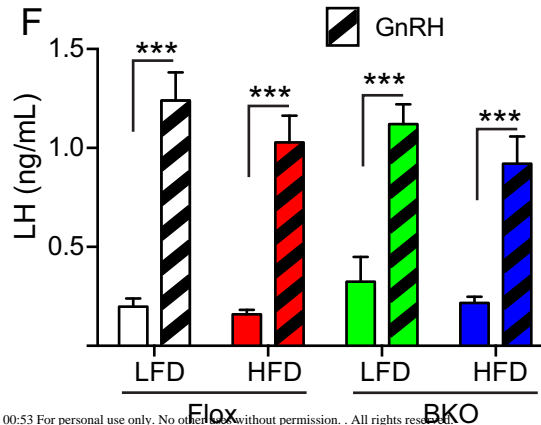
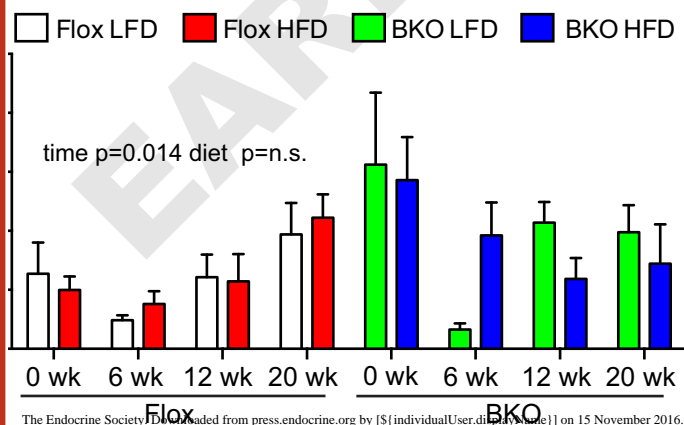
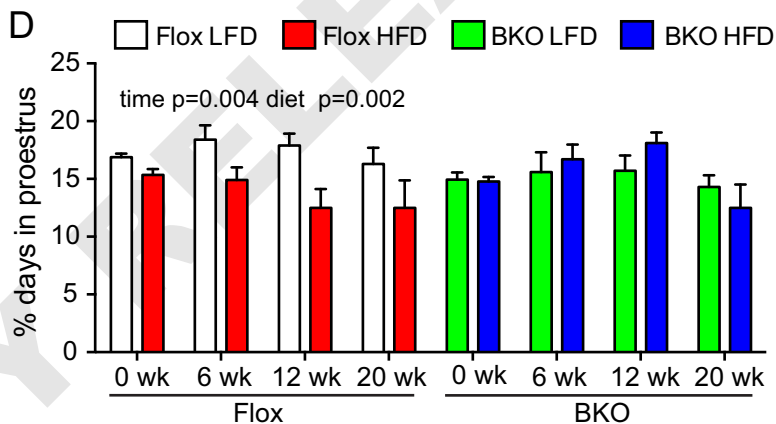
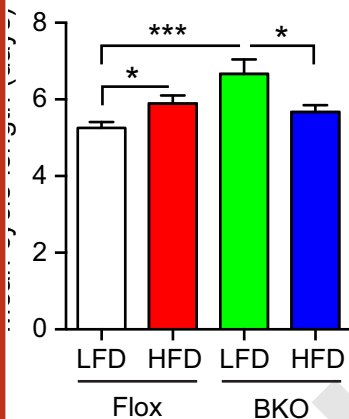
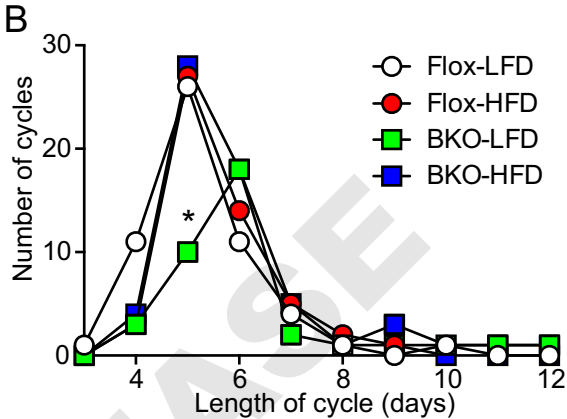
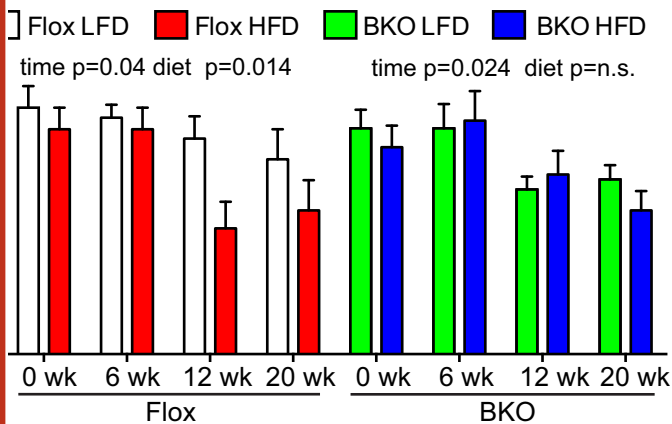


F

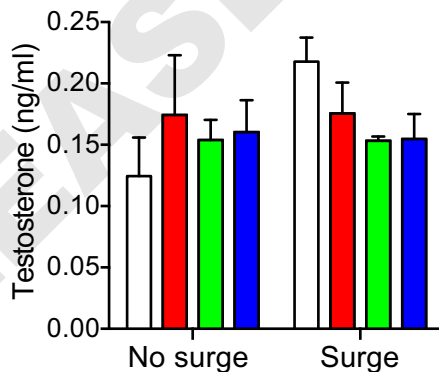
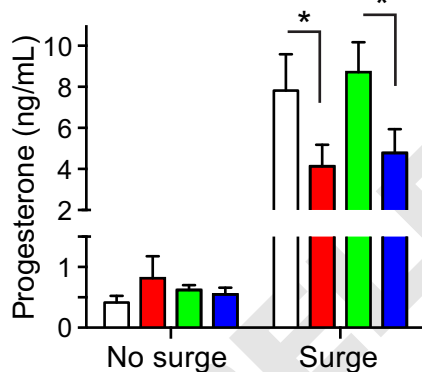
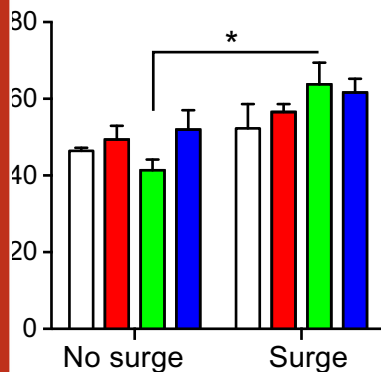


C



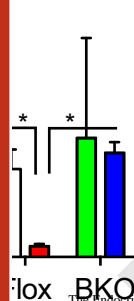


□ Flox before    ■ Flox HFD    ■ BKO before    ■ BKO HFD

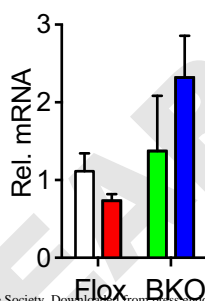


□ Flox LFD    ■ Flox HFD    ■ BKO LFD    ■ BKO HFD

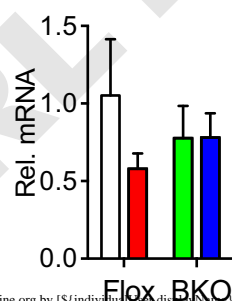
*yp19a1*



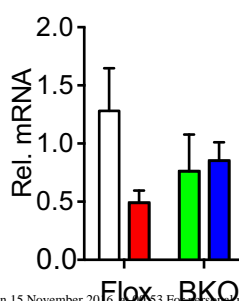
*Hsd17b1*



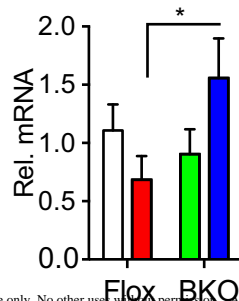
*Star*



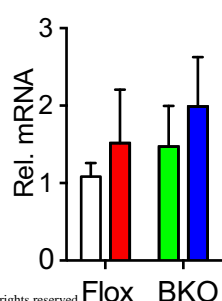
*Hsd3b1*



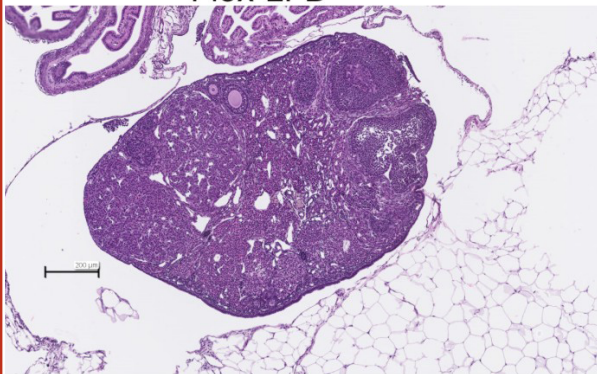
*Cyp11a1*



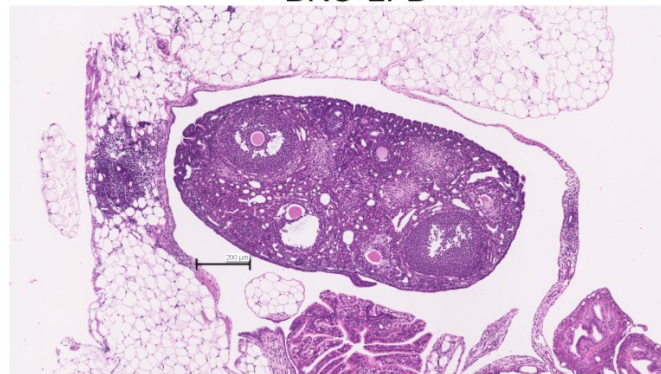
*Cyp17a1*



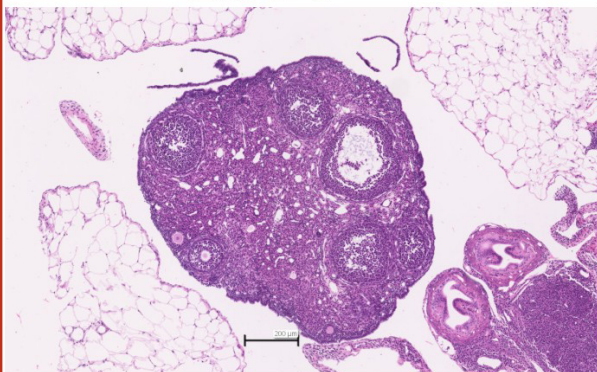
Flox-LFD



BKO-LFD



Flox-HFD



BKO-HFD

